Journal of Rock Mechanics and Geotechnical Engineering 15 (2023) 2868–2876

Contents lists available at ScienceDirect

Journal of Rock Mechanics and Geotechnical Engineering

journal homepage: www.jrmge.cn

Full Length Article

Spatial deduction of mining-induced stress redistribution using an optimized non-negative matrix factorization model

Xu-yan Tan [a,b], Weizhong Chen [a,b,*], Luyu Wang [c], Changkun Qin [a,b]

[a] State Key Laboratory of Geomechanics and Geotechnical Engineering, Institute of Rock and Soil Mechanics, Chinese Academy of Sciences, Wuhan, 430071, China
[b] University of Chinese Academy of Sciences, Beijing, 100049, China
[c] Department of Civil and Environmental Engineering, The Hong Kong Polytechnic University, Hung Hom, Kowloon, Hong Kong, China

ARTICLE INFO

Article history:
Received 15 September 2022
Received in revised form
25 October 2022
Accepted 7 December 2022
Available online 9 January 2023

Keywords:
Machine learning
Underground construction
Monitoring
Mining-induced stress
Prediction

ABSTRACT

Investigation of mining-induced stress is essential for the safety of coal production. Although the field monitoring and numerical simulation play a significant role in obtaining the structural mechanical behaviors, the range of monitoring is not sufficient due to the limits of monitoring points and the associated numerical result is not accurate. In this study, we aim to present a spatial deduction model to characterize the mining-induced stress distribution using machine learning algorithm on limited monitoring data. First, the framework of the spatial deduction model is developed on the basis of non-negative matrix factorization (NMF) algorithm and optimized by mechanical mechanism. In this framework, the spatial correlation of stress response is captured from numerical results, and the learned correlation is employed in NMF as a mechanical constrain to augment the limited monitoring data and obtain the overall mechanical performances. Then, the developed model is applied to a coal mine in Shandong, China. Experimental results show the stress distribution in one plane is derived by several monitoring points, where mining induced stress release is observed in goaf and stress concentration in coal pillar, and the intersection point between goaf and coal seam is a sensitive area. The indicators used to evaluate the property of the presented model indicate that 83% mechanical performances have been captured and the deduction accuracy is about 92.9%. Therefore, it is likely that the presented deduction model is reliable.

1. Introduction

With the rapid construction of deep large-scale projects, the problem of long-term stability and dynamic disaster prevention in deep energy exploitation has become increasingly prominent (Mohammad et al., 2015; Wang et al., 2022). Actually, the problem is related to mining-induced stress redistribution during the coal mining because the excavation of chamber in the intact rock mass could induce large movement of overlying rock (Kang et al., 2018; Wang et al., 2020). The in situ stress of rock mass would transfer to the surrounding area and change the stress distribution, particularly the location ahead the working face. It is well recognized that the solution for the mining-induced stress redistribution is the key to ensure the safety excavation of deep mining (Kaiser et al., 2001; Xie et al., 2011). However, the traditional methods based on elastoplastic mechanics theory have limits such as complicated solution process and large influence of rock heterogeneity (Cheng et al., 2022). With the development of computer science, structural health monitoring (SHM) system has been widely used in coal seam and the data-driven methods are adopted to solve the problem of stress redistribution (Adam, 2021; Prasanjit et al., 2021). Due to the complex working conditions and limited monitoring points, SHM data are sometimes sparse or even missing, resulting in insufficient perception of the overall stress distribution (Tan et al., 2021a; Zhu et al., 2022). Therefore, it has always attracted the attention of mining engineers to understand the abutment pressure distribution around mining face. For this, this study aims to develop a spatial deduction model driven by the mechanism and monitoring data to characterize the mining-induced stress redistribution on the overall roof of coal seam.

* Corresponding author. State Key Laboratory of Geomechanics and Geotechnical Engineering, Institute of Rock and Soil Mechanics, Chinese Academy of Sciences, Wuhan, 430071, China.
E-mail address: wzchen@whrsm.ac.cn (W. Chen).

Peer review under responsibility of Institute of Rock and Soil Mechanics, Chinese Academy of Sciences.

https://doi.org/10.1016/j.jrmge.2022.12.008
1674-7755

Over the past few years, great efforts have been made to solve the problem of mining-induced stress redistribution (e.g. Wang et al., 2020). Some representative achievements include Protodyakonov theory (Protodyakonov, 1907) and Fenner solution (Fenner, 1938), the principle of effective stress presented by Terzaghi (1943), Caquot formula (Caquot and Kérisel, 1948), Kastner solution (Kastner, 1971), and the key stratum in ground control presented by Qian (1984). Most of the classical methods used to solve the stress redistribution problem are developed on the basis of the elastoplastic theory. But it is difficult to define the cell body due to the size effect of rock mass. In addition, the cell cube is usually assumed to be continuous and homogeneous (Zhang et al., 2020), which ignores the anisotropic effect of rock mass. To this end, the probabilistic model is regarded as a new method to characterize the mining-induced stress redistribution since both the discontinuous tangential stress and supporting pressure produce a complicated evolution process from in situ stress to stress increase, stress release, and failure at a macroscopic scale (Wang et al., 2019; Rami et al., 2020). Correspondingly, the statistical models such as Weibull distribution, Gumbel distribution, and Gamma distribution were adopted to describe the evolution process of rock mass, based on which the stress distribution models were developed in macroscopic scale (Cao et al., 2022; Gonzalez et al., 2022). However, the solution obtained from the probabilistic model is not robust due to the lack of modeling data and the incompact integration with mechanical mechanism.

With the development of big data technology, machine learning on SHM data (ML-SHM) is regarded as a reliable method to obtain the mechanical state of structure (Du et al., 2021; Mohammad et al., 2021; Tan et al., 2022a). The ML-SHM method has been widely used in the data analysis of many underground and subsurface facilities, such as tunnel engineering, pit engineering, and landslide engineering (Li et al., 2022). This method has played an important role in monitoring signal processing, anomaly detection, and structural mechanical behavior prediction (Tan et al., 2020; Prosper et al., 2022). Unfortunately, the monitoring data are sometimes inaccurate because the sensors used to collect the stress data are usually installed in the cracked coal seam (Qin et al., 2022). For example, the monitoring for stope is restricted by the number of monitoring points, which brings a challenge to perceive the redistribution property of mining-induced stress in the stope. In fact, the insufficient perception for the overall mechanical behaviors of the structure occurs in many fields. At present, it has become an important solution to dynamically reconstruct the structural mechanical response using matrix as the intermediate variable, which has been applied and verified in the loss signal recovery of wireless system, temperature signal reconstruction, monitoring of global air quality, and other fields (Teng et al., 2019). It has also been proved that non-negative matrix factorization (NMF) is superior in dimension transformation, based on which the limited time series of monitoring data could be used to derive a multi-dimensional matrix representing the mechanical variation of more spatial positions (Ludeña-Choez et al., 2019).

To this end, this study aims to present a spatial deduction model to perceive the mining-induced stress of overall coal roof in view data-driven point. As a case study, the presented model is employed in the coal mine to perceive the mining-induced stress of a panel and prevent disasters in advance. This study is supposed to promote the development of intelligent construction in the field of coal mining.

2. Spatial deduction model for the mining-induced stress

2.1. Framework of spatial deduction model

Restricted by the limited number of monitoring points in the field, it is impossible to perceive the response of mining-induced stresses of overall walls and that ahead of the working face (which are referred to as the overall mining-induced stress). This section aims to develop a spatial deduction model to characterize the overall response of mining-induced stresses on the basis of limited monitoring information. The flowchart of the presented model is displayed in Fig. 1. Clearly, the spatial deduction model mainly consists of three components, data-driven model fusing on NMF algorithm, numerical simulation, and model optimization. The mechanical correlations captured from numerical results are embedded into NMF model to optimize the data-driven model.

First, the roof of coal mine is represented by a matrix, where the roof is separated into infinitesimal elements and each element has a corresponding unit in the matrix. The matrix is sparse because only the units corresponding to the elements where the monitoring points are arranged have the values, and the rest are null. Therefore, the problem of spatial deduction for mining-induced stress is transformed into imputing the null values of matrix via the sparse values. Obviously, this problem can be solved if the correlation between the units in the matrix is obtained. For this, the numerical simulation is used to learn the spatial distribution characteristics of mining-induced stress and capture the spatial correlations preliminary. Then, a matrix with values is derived according to the spatial correlations. Finally, the error between the deduced results with actual monitoring data is used to inverse the parameters in deduction model. If the error is the smallest, the procedure would terminate and the calculated result of matrix is the spatial mining-induced stress (Tan et al., 2021b). The methodology of each component is introduced as follows.

2.2. Data-driven model fusing on NMF

Supposing a plane in the coal mine roof is separated into m layers in y-axis and n layers in x-axis, as shown in Fig. 2, the corresponded sparse matrix is generated, $\boldsymbol{X} \in R^{m \times n}$, where the j th element in the i th row of the plane corresponds to the unit of (i,j) in the matrix. It has been proved that NMF is superior to capturing the core features of data in the matrix and calculate their weights respectively, so this algorithm is adopted to impute the empty units in the sparse matrix in this study. The values in the empty units can be derived by reducing the dimension of the sparse matrix and reconstructing it. For the sparse matrix $\boldsymbol{X} \in R^{m \times n}$, NMF approximates it through two low rank matrices $\boldsymbol{W}$ and $\boldsymbol{F}$ (Ludeña-Choez et al., 2019):

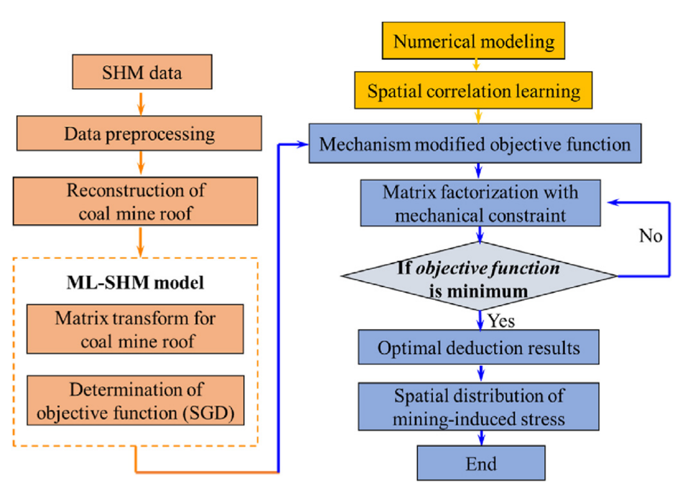

Fig. 1. Flowchart of the presented spatial deduction model (SGD: Stochastic gradient descent).

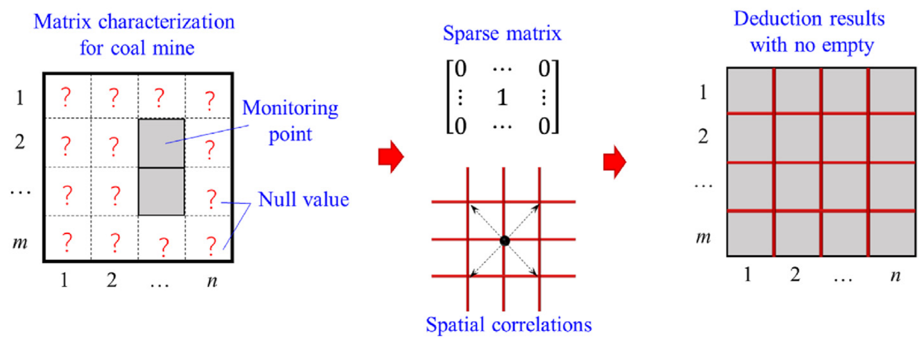

Fig. 2. Formalization of NMF model on the roof of coal mine.

$$\boldsymbol{X} \approx \boldsymbol{W}\boldsymbol{F} \tag{1}$$

where $\boldsymbol{W} \in R^{m \times h}$ is the weight matrix, $\boldsymbol{F} \in R^{h \times n}$ is the feature matrix, and $h \leq \min(m, n)$ is the converted dimension.

Based on these two matrices, a dense matrix with no null value would be reconstructed. In this model, the SGD is adopted to learn $\boldsymbol{W}$ and $\boldsymbol{F}$, and $L2$ regularization is applied in the loss function. However, due to the complex geological conditions of coal mine, the constraints on these two matrices are not sufficient, and the boundary conditions need to be considered. Therefore, it is essential to introduce the mechanical mechanism to modify the simple $L2$ regularization.

2.3. Optimization for NMF model

2.3.1. Analysis for the mining-induced stress distribution

The existing studies have indicated that the stresses in the front and two sides of the working face have similar variation trend. As the distance from the working face increases, the stress increases significantly at first, then decreases, and finally stabilizes, as shown in Fig. 3a. This is a macroscopic reflection of crack development during mining, rather than a random phenomenon. Furthermore, the distribution characteristics of mining-induced stress reflect the whole evolution trend of crack, from initial crack, close and expand, local link, to entirely crack link, which correspond to the in situ stress zone, slightly disturbed zone, violently disturbed zone, and stress relief zone (Wang et al., 2019), as shown in Fig. 3b. Then, some statistical models are used to describe the evolution trend of mining-induced stress, and it is found that Weibull formula is one of the commonly used methods (Vitor and Claudio, 2020). Two parameters, k and ω, are used to determine the shape and magnitude of a Weibull curve. The recommended form of Weibull formula is as follows:

$$\sigma_z(x) = \frac{k}{\omega}\left(\frac{x}{\omega}\right)^{k-1} \exp\left[-\left(\frac{x}{\omega}\right)^{k}\right] \tag{2}$$

where σ_z represents the vertical stress of coal mine roof, and x represents the distance to the free face.

The values of parameters k and ω are close to the spatial positions. For example, the values at point a are different to that at point b due to the distance difference to the coal pillar, which means that a single Weibull formula is suitable to describe the distribution characteristics of mining-induced stress in one direction but insufficient to characterize the overall stress in one plane. However, it is impossible to obtain the spatial Weibull curves when only rely on the limited monitoring data as they are of a local area. To this end, the numerical model is adopted to simulate the overall distribution characteristics of mining-induced stress. Based on the simulated data, the spatial correlations of mining-induced stress in the overall roof can be captured and described by Weibull formula with variable parameters.

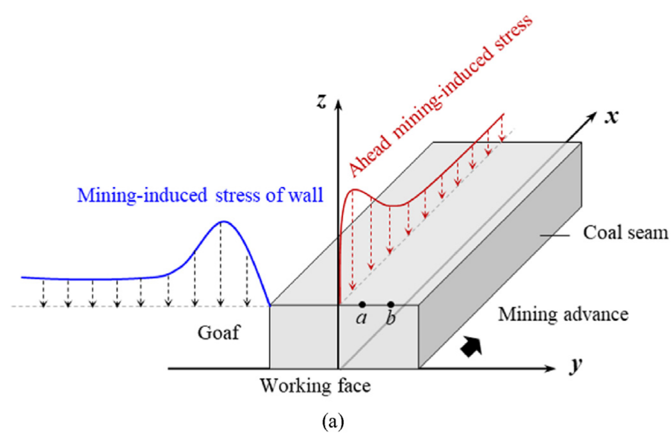

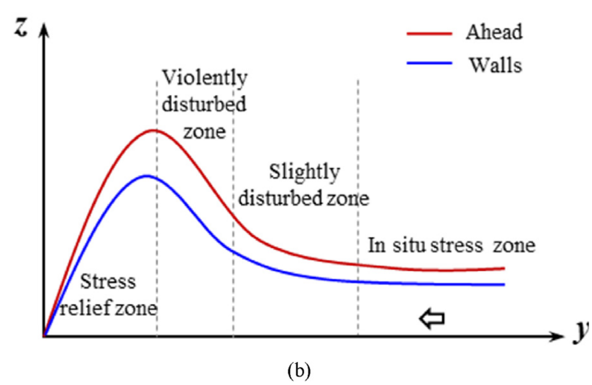

Fig. 3. Schematic diagrams of the mining-induced stress redistribution: (a) Spatial distribution of mining-induced stress; and (b) Whole evolution trend of stress.

2.3.2. Modified objective function

The objective function is used to train an optimized model with minimum error. In this study, it is used to make the deduced result of stress as approaching as possible to the actual situation. The recommended form of traditional objective function obj' is as follows:

$$obj' = \sum_{(i,j)\in\mathbb{A}} \left\| \boldsymbol{X}_{i,j} - \boldsymbol{W}_{i,:} \bullet \boldsymbol{F}^{\mathrm{T}}_{:,j} \right\|^2 \tag{3}$$

where $\boldsymbol{W}_{i,:}$ is the ith row vector, $\boldsymbol{F}_{:,j}^{\mathrm{T}}$ is the transposition of jth column vector, and $\mathbb{A}$ is the subscript set of non-empty unit in the matrix.

According to the analytical results of mining-induced stress distribution, a modified objective function considering the spatial correlation of mechanical response is introduced in this study. This item is used to make the deduced result to as approach the Weibull formula. Using Eq. (3), the modified objective function is given as follows:

$$obj = \sum_{(i,j)\in\mathbb{A}} \left\| X_{i,j} - W_{i,:} \bullet F_{:,j}^{\mathrm{T}} \right\|^2 + \gamma_1 \sum_{i=1}^{M}\sum_{j=1}^{N} \left\| X_{i,j} - \sigma_z \right\|^2 \tag{4}$$

where $\gamma_1 \sum_{i=1}^{M}\sum_{j=1}^{N}\left\|X_{i,j}-\sigma_z\right\|^2$ is the item of boundary condition constraint, and γ_1 is a hyper-parameter used to balance the weight of the mechanical constraint.

In order to evaluate the deduction capability, three evaluation indicators are adopted in this study, i.e. root mean square error (RMSE), mean absolute percentage error (MAPE), and Pearson correlation coefficient (PCC). Specifically, RMSE is used to measure the deviation between the deduction value and the actual data (Tan et al., 2022b):

$$RMSE = \sqrt{\frac{1}{n}\sum_{i=1}^{n}(y_i - \widehat{y}_i)^2} \tag{5}$$

where y_i and $\widehat{y}_i$ are the actual data and deduction results, respectively.

MAPE is a dimensionless indicator to measure the ratio of absolute error to the ground truth, which can be used to describe the deduction accuracy of the presented model. It is calculated as follows:

$$MAPE = \frac{100\%}{n}\sum_{i=1}^{n}\left|\frac{y_i - \widehat{y}_i}{y_i}\right| \tag{6}$$

PCC is used to measure the correlation of deduction results with ground truth. Its value represents the learning ability of the deduction model to the variation trend of stress data. The larger value means the stronger correlation between the deduction results and the actual data. The calculation formula is

$$PCC = \frac{\sum_{i=1}^{n}(y_i - \overline{y}_i)(\widehat{y}_i - \overline{\widehat{y}}_i)}{\sqrt{\sum_{i=1}^{n}(y_i - \overline{y}_i)^2\sum_{i=1}^{n}(\widehat{y}_i - \overline{\widehat{y}}_i)^2}} \tag{7}$$

where $\overline{y}_i$ and $\overline{\widehat{y}}_i$ are the average values of actual data and deduction results, respectively.

3. Field monitoring for a study case

3.1. Geological and mining conditions

A panel of coal mine, located in Jining, Shandong Province, China is selected as study case. The overburden of this panel is about 661.2 m, and the length and width are 1400 m and 245 m, respectively. The mining conditions in the site are displayed in Fig. 4, where haulage roadway and ventilation roadway, with a width of 5 m are pre-extracted.

In addition, the geological layer of panel immediate roof is mudstone with an average depth of 0.8 m. The main roof is comprised of fine-grained sandstone, with an average depth of 12.9 m. The immediate floor of the panel is siltstone with a depth of 1.54 m. The main floor consists of fine-grained silt-stone with an average depth of 7.7 m. The detailed geological conditions of the overlying rock are shown in Fig. 5, and the mechanical properties of different geological layers are listed in Table 1.

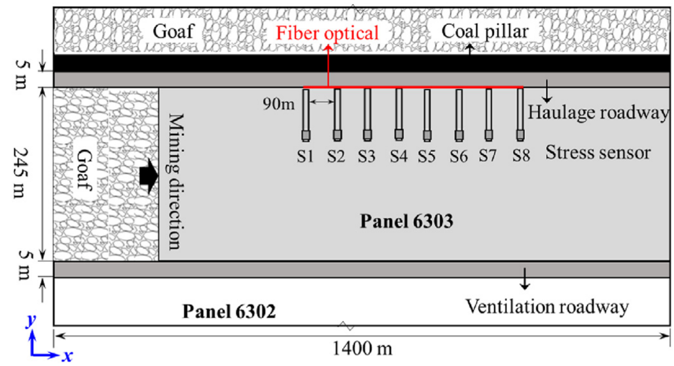

Fig. 4. Mining conditions of Dongtan coal mine.

3.2. Monitoring scheme in the site

Due to the effect of high stress distribution around the mining area, the microseismic events occurred frequently in this panel during the extraction process. In order to capture the mechanical behaviors of the roof rock, some stress sensors are installed in the field. Different to the traditional monitoring scheme, the sensors are installed in the intact and homogenous main roof rather than soft coal seam (Fig. 6), which reduces the installation difficulties of drilling and ensures the reliability of monitoring data. The details of the stress sensors and its installation technology can be found in Zhao et al. (2020). In Fig. 4, a total of 8 monitoring points (S1 to S8) is determined in the site and the distance between every two monitoring points is 90 m along the mining advance direction. The drilling is inclined about 35° with a depth of 15–20 m. Each sensor records the stress changes within 120 m ahead of the working face with a sampling interval of 3 m.

According to the designed monitoring scheme, the average stress variation recorded by several sensors is calculated, as displayed in Fig. 7, where σ_{xx} is the stress along strike direction, σ_{yy} is the stress along dip direction, and σ_{zz} is the normal stress. It can be found that the stresses increase with the approach of working face.

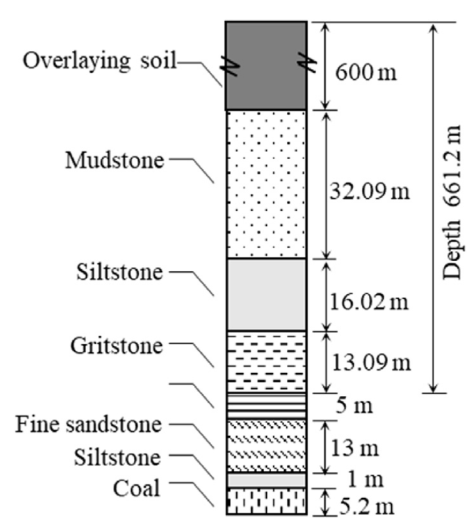

Fig. 5. Geological layers of overlying rock.

Table 1
Property parameters of different geological layers.

Geological layers	Bulk modulus (GPa)	Shear modulus (GPa)	Density (kg/m^3)	Cohesion (MPa)	Internal friction angle (°)
Siltstone	12.88	6.64	2500	5.5	24
Medium-sandstone	12.41	8.93	2800	6.4	25
Fine stone	9.84	8.01	2780	5.7	23.8
Gritstone	17.2	11.84	2855	6.2	32
Coal	1.77	1.44	2410	2.3	27
Mudstone	6.31	3.97	2400	3.2	32.6
Overlaying soil	13.33	8	2510	6	24

In addition, the response of stress varies in different directions, and that of z-axis is largest. The study focuses on the analysis of mining-induced stress in vertical direction, which reflects the mechanical state of the coal mine roof in order to prevent mining disasters.

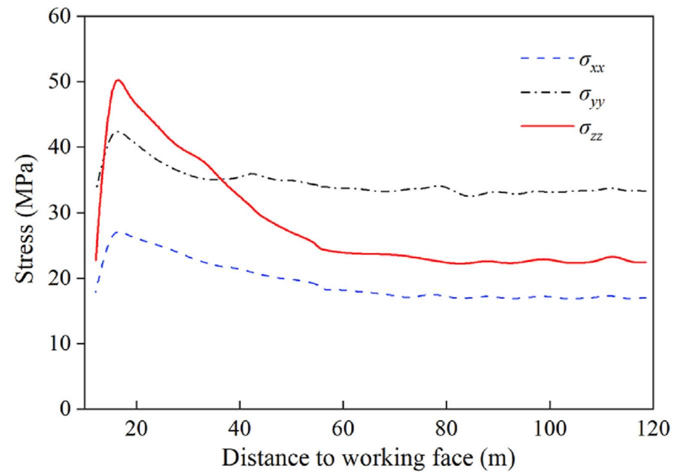

Fig. 7. Monitoring results of mining-induced stress ahead of the working face.

4. Spatial response correlations of mining-induced stress

Although the numerical result is rough to describe the magnitude of mining-induced stress, the spatial correlations of mechanical responses in the calculated results are important. To this end, a numerical model is developed to obtain the mining-induced stress dataset to capture the spatial correlations.

4.1. Numerical modeling of mining-induced stress

In order to understand the impact of mining on stress redistribution, especially that on the goaf, the finite difference method is adopted for modeling (Mikhail et al., 2020; Dakshith et al., 2022). According to the geological conditions in the field, the size of the numerical model is 270 m × 450 m × 260 m, where the strike length is 270 m, the dip length is 450 m, and the height is 260 m. In addition, the width of the working face is 245 m, the width and height of roadways are 5 m, and the widths for the goaf and entitative coal seam are 100 m and 95 m, respectively. In this model, the solid elements are adopted to simulate the mechanical behavior of stope, and the Mohr-Coulomb formula is adopted to simulate the plastic behavior. The developed numerical model of the study case is displayed in Fig. 8.

In order to calculate the mechanical response of mining-induced stress, the stress in the vertical direction is arranged on the roof of coal mine:

$$F = \sum_{i=1}^{l} \varphi_i h_i \tag{9}$$

where l is the number of geological layers of overlying rock, φ_i and h_i represent the unit weight and height of layer i, respectively.

Furthermore, the fixed constraints are applied on the surfaces of bottom, left and right, front and back. According to the results of in situ rock stress testing in the field, the lateral pressure coefficients at x- and y-axis of the coal mine roof are determined as 0.8 and 1.4, respectively.

4.2. Analysis of the numerical results

Using the developed model, the mining-induced stress distribution on the panel roof can be obtained. For example, the numerical result of stress in the plane where the monitoring points are arranged is extracted, as shown in Fig. 9. Obviously, the stresses in the front and two sides of the working face are larger than that in other positions, and the stress decreases gradually with increase of the distance from the working face. Furthermore, the mining-induced stress at the side of the goaf is greater than that at the solid coal, which denotes that the goaf has great influence on the mining-induced stress redistribution.

Specially, the evolution trend of mining-induced stress is derived, as shown in Fig. 10. Fig. 10a shows the stress distribution along the strike direction, and Fig. 10b and c shows the stress

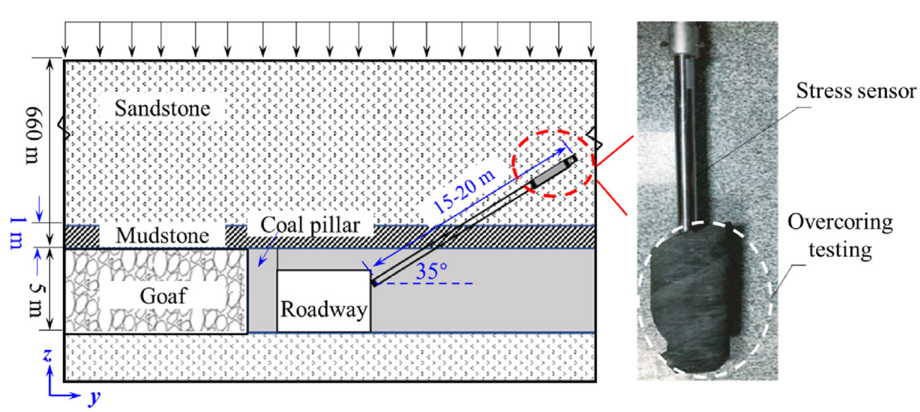

Fig. 6. Sketch map of FBG sensor installation.

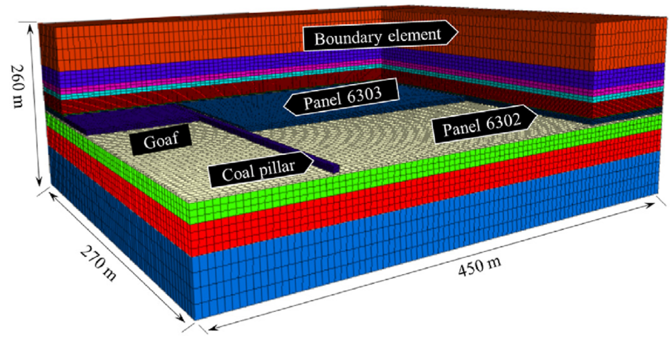

Fig. 8. The numerical model a panel in coal mine.

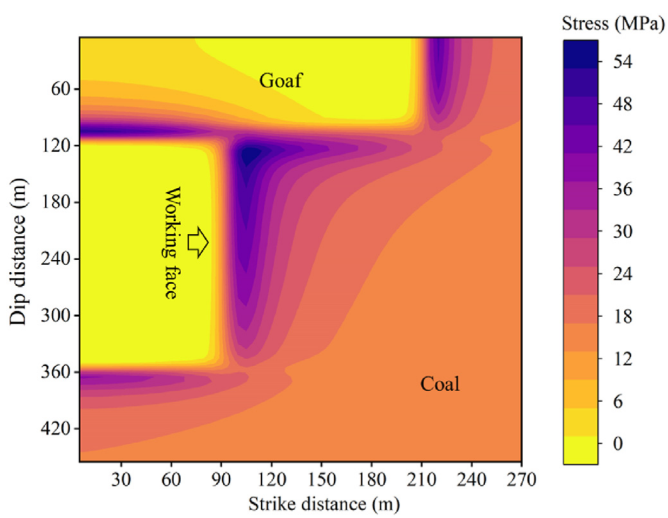

Fig. 9. Spatial distribution of mining-induced stress characterized by numerical results.

distribution along the dip direction. It can be found that the mining-induced stress distribution agrees with Weibull distribution features. In the statistical model formalized on the numerical data, the Weibull formula is described with red lines. The shape parameter k and magnitude parameter ω are derived, which vary with different positions. Therefore, the distribution characteristic of mining-induced stress can be described using the Weibull formula, and used to derive the values of k and ω at different positions of the overall coal mine roof.

4.3. Spatial correlation using numerical results

Based on the stress distribution obtained from numerical model, this section aims to derive the spatial correlation of stress response using Weibull formula. It has been proved that the mining-induced stress obeys the Weibull formula in both of the strike and dip directions. Therefore, the spatial correlations of mining-induced stress in the front and sides of working face can be captured separately according to Eq. (2). When the indexes of the divided elements are defined according to Fig. 11, the Weibull formula in the front of working face is formalized as

$$\sigma_{i\in(r1:r2),j}(x) = \frac{k}{\omega}\left(\frac{x}{\omega}\right)^{k-1} \exp\left[-\left(\frac{x}{\omega}\right)^{k}\right] \tag{10}$$

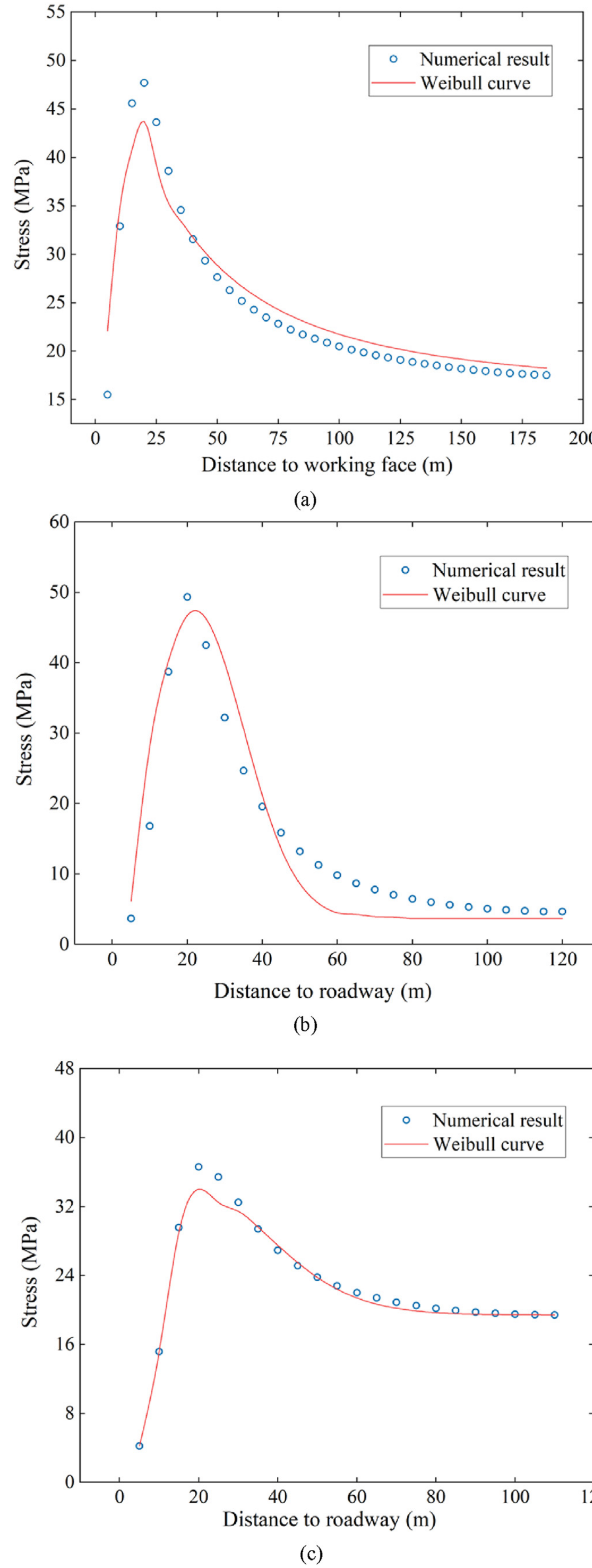

Fig. 10. Evolution trend of the mining-induced stress in (a) Front; (b) Goaf side; and (c) Unexploited side.

where $r1$, $r2$ are the beginning and ending index of the raw in front of working face, which are set to be 35 and 117 in this experiment.

Similarly, the Weibull formula of the side is formulated as follows:

$$\sigma_{i\in(1:r1,r2:r),j}(y)=\frac{k}{\omega}\left(\frac{y}{\omega}\right)^{k-1}\exp\left[-\left(\frac{y}{\omega}\right)^{k}\right] \tag{11}$$

where r is the number of rows in the plane that are divided, and set to 150; and y is the distance from the working face in the direction perpendicular to mining advance.

According to Eqs. (10) and (11), the spatial correlations of mining-induced stress in the overall roof of coal mine are captured. The learned correlations would be adopted to optimize the NMF model to deduce the in situ mining-induced stress.

5. Model application to the dongtan coal mine

5.1. Data preprocessing and model preparation

The monitoring data obtained in the study case is adopted to verify the presented model. As mentioned above, the sensor collects data every 3 m of excavation and each sensor can record the stress distribution within 120 m, so 40 monitoring data are recorded by one sensor. Correspondingly, the plane that the sensor installed is divided into the element with side length of 3 m, as shown in Fig. 11. The method for assigning the monitoring value to the corresponding units in the matrix is available in Appendix A. Consequently, the indexes of the units corresponding to the monitoring data are calculated by

$$\mathbb{A}_{i,j}, i=40, j\in[27:67] \tag{12}$$

Overfitting is a common problem in machine learning, which is mainly caused by the pursuit of minimizing the error between the calculated results and the truth values. In order to avoid the overfitting problem, the recorded data is randomly divided into three datasets, i.e. training set $\mathbb{A}_{\text{tr}}$, testing set $\mathbb{A}_{\text{te}}$, and validation set $\mathbb{A}_{\text{va}}$ according to the approximate ratios of 0.7, 0.2, and 0.1. The data in the training set and testing set are used for calculation, while the data in the validation set are used for model verification. Therefore, the objective function is performed according to Eqs. (4), (10) and (11), which is formalized as follows:

$$obj=\sum_{(i,j)\in\mathbb{A}_{tr},\mathbb{A}_{va}}\left\|X_{i,j}-W_{i,:}F_{:,j}^{\mathrm{T}}\right\|^2+\gamma_1\sum_{i=35}^{117}\times\sum_{j=27}^{90}\left\|X_{i,j}-\sigma(x)\right\|^2+\gamma_2\sum_{i=1,}^{33}\sum_{j=1}^{90}\left\|X_{i,j}-\sigma(y)\right\|^2+\gamma_3\sum_{i=119,}^{150}\times\sum_{j=1}^{90}\left\|X_{i,j}-\sigma(y)\right\|^2 \tag{13}$$

where γ_2 and γ_3 are the hyper-parameters used to balance the weight of Weibull constraint.

Considering the length of divided element is 3 m, x and y can be calculated as follows:

$$x=3^*i;\ y=3^*j \tag{14}$$

According to the pre-trained spatial correlation on numerical results and the limited monitoring data in the field, the redistribution of mining-induced stress is derived in Fig. 12. It can be found that the distribution characteristics of mining-induced stress obtained from the deduction model are consistent with that obtained from numerical simulation.

5.2. Discussion for the spatial deduction results

In order to verify the reliability of the spatial deduction model, the numerical results are adopted to compare with the deduction results. The calculation results corresponding to the positions where the monitoring information is recorded are shown in Fig. 13. Obviously, these three curves follow the same trend, while the variation magnitude is different. In contrast to the numerical result, the error of deduction result is smaller because the stress curve of the deduction result is closer to that of the actual monitoring result. It is indicated the necessity to present such ML-SHM model although numerical simulation can be used to deduce the mechanical behavior of the overall roof. Therefore, the presented spatial deduction model is reasonable to obtain the mining-induced stress of the coal mine roof.

Inputting the monitoring data in validation set and the corresponding deductions into Eq. (5)–(7), it shows that the calculated

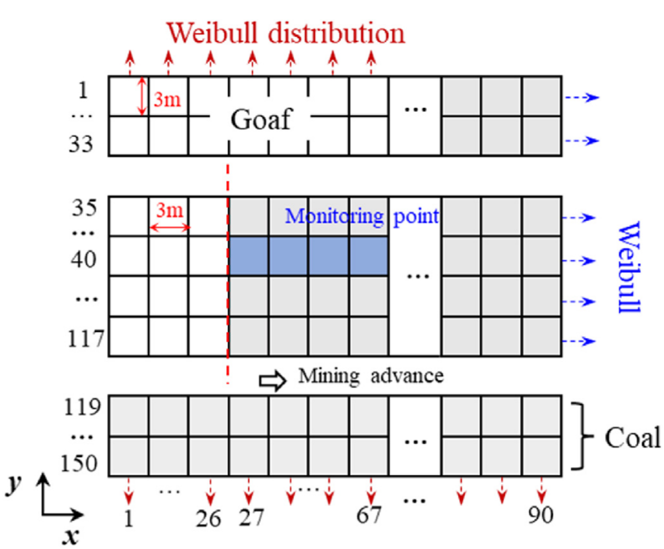

Fig. 11. Indexes of each unit in the matrix.

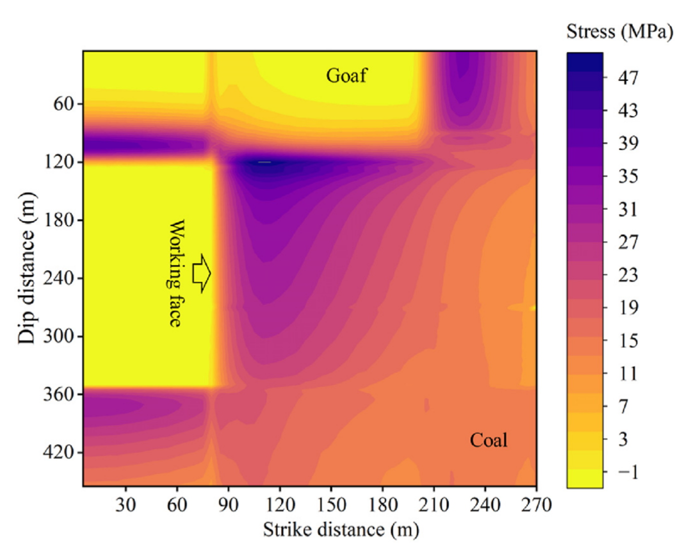

Fig. 12. Deduction result of the mining-induced stress.

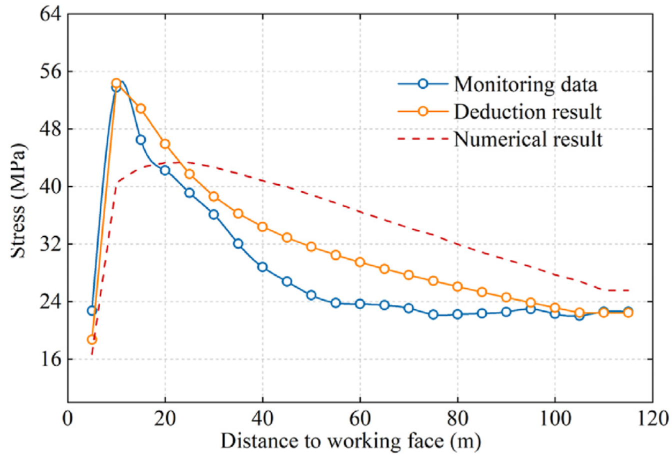

Fig. 13. Comparison of deduction results with actual monitoring data.

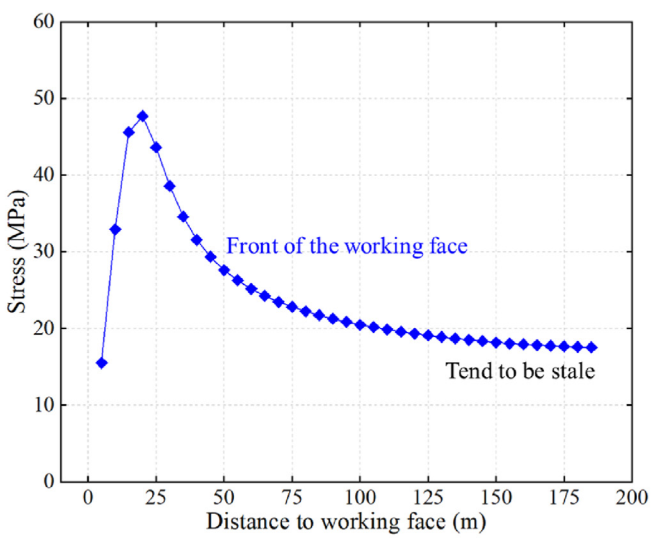

(a)

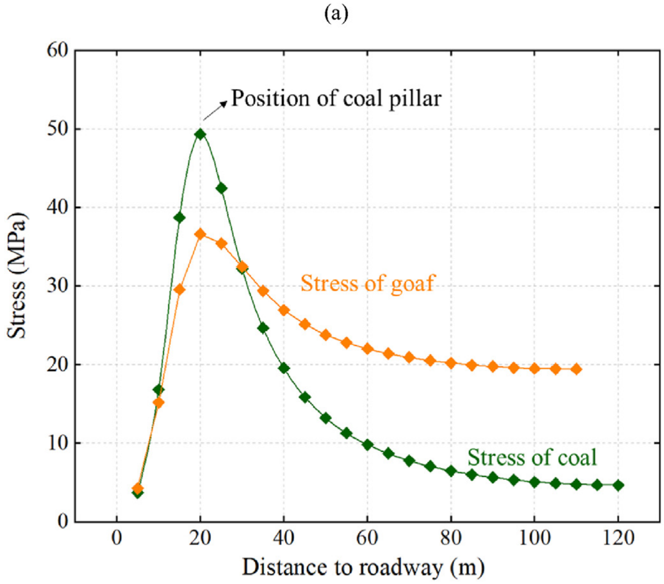

(b)

Fig. 14. Mining-induced stress of some positions in site (a) Front and (b) Goaf side.

values of PCC, RMSE, and MAPE are 83%, 3.14 MPa, 92.9%, respectively. This indicates that 83% mechanical characteristics have been captured by the spatial deduction model. The error between the deduction results with actual monitoring data is less than 3.14 MPa, and the deduction accuracy is about 92.9%. Therefore, the presented model is reliable.

5.3. Application of the actual mining-induced stress

According to the deduction results in Fig. 12, the stress response to coal mining can be analyzed. Three stress distribution curves located in the front of working face, goaf and unexploited coal seam are extracted from the deduction results, as displayed in Fig. 14. The deduction results denote that the stress in coal seam increases suddenly and then drops to stable, and the trend values of both them are close to 20 MPa. Compared to the stresses of two sides, the location of maximum stress is different. The maximum value of mining-induced stress at the goaf side is located at the coal pillar rather than the goaf roof. Furthermore, the stable stress value of goaf roof is about 5 MPa, which is far less than that of coal seam.

In summary, coal mining induces stress release of goaf and stress concentration of coal pillar, and the maximum value of the concentrated stress is nearly 50 MPa. In order to ensure the safety of coal mine, it is essential to reserve coal pillar with sufficient width. Furthermore, the in situ stress of coal mine is about 20 MPa and the sensitive area of roof is the intersection of goaf and coal seam in front of working face, which is the essential location to arrange sensor.

6. Conclusions

In this study, a spatial deduction model was presented to characterize the mining-induced stress distribution through NMF algorithm using sparse monitoring data. The presented model is used to solve the problem of insufficient perception of the stress state of the roof, and provide guidance to ensure the safe operation of underground engineering.

There are strong spatial correlations in the structural mechanical response, which were precaptured on the numerical dataset. The mining-induced stress distribution in front of working face satisfies Weibull formula. Then an integrated model is presented to characterize the spatial distribution of mining-induced stress, where the mechanical correlations captured from numerical results are embedded into NMF model to optimize the pure data-driven model. The deduction results shown that the goaf has a significant influence on the redistribution of mining-induced stress, which induces stress release of goaf and stress concentration of coal pillar.

As a study case, the presented model is formalized on the mine coal to characterize the mining-induced stress of the overall roof. Compared to the numerical results, the deduction results agree well with the actual monitoring data, where 83% mechanical characteristics have been captured and the accuracy is about 92.9%. Therefore, the presented model is reasonable and it would play a great role in promoting the smart management of coal mining.

Declaration of competing interest

The authors declare that they have no known competing financial interests or personal relationships that could have appeared to influence the work reported in this paper.

Acknowledgements

This work is supported by the National Natural Science Foundation of China (Grant No. 51991392), Key deployment projects of Chinese Academy of Sciences (Grant No. ZDRW-ZS-2021-3), Project for Research Assistant of Chinese Academy of Sciences, and National Key R&D Program of China (Grant No. 2021YFC3100805).

Appendix A. Supplementary data

Supplementary data to this article can be found online at https://doi.org/10.1016/j.jrmge.2022.12.008.

References

Adam, L., 2021. Spatio-temporal hierarchical cluster analysis of mining-induced seismicity in coal mines using Ward's minimum variance method. J. Appl. Geophys. 184, 104249.
Cao, K.W., Ma, L.Q., Wu, Y., et al., 2022. Statistical damage model for dry and saturated rock under uniaxial loading based on infrared radiation for possible stress prediction. Eng. Fract. Mech. 260, 108134.
Caquot, A., Kérisel, J.L., 1948. Tables for the Calculation of Passive Pressure, Active Pressure and Bearing Capacity of Foundations. Gautier-Villars, Paris.
Cheng, G., Xu, W.T., Shi, B., Wu, J.H., Sun, B.Y., Zhu, H.H., 2022. Experimental study on the deformation and failure mechanism of overburden rock during coal mining using a comprehensive intelligent sensing method. J. Rock Mech. Geotech. Eng. 14 (5), 1626–1641.
Dakshith, R.W., Ashley, D., Greg, Y., Khandelwal, M., Song, C.M., Ooi, E.T., 2022. Development of the scaled boundary finite element method for image-based slope stability analysis. Comput. Geotech. 143, 104586.
Du, B.W., Li, W.T., Tan, X.Y., Ye, J.C., Chen, W.Z., Sun, L.L., 2021. Development of load-temporal model to predict the further mechanical behaviors of tunnel structure under various boundary conditions. Tunn. Undergr. Space Technol. 116, 104077.
Fenner, R., 1938. Untersuchungen zur erkenntnis des gebirgsdruckes. Gluckauf 32, 681–695 (in German).
Gonzalez, F.J., Vallejosa, J.A., Rojas, E., 2022. Evaluation of the seismic rock mass response to mining and the impact of preconditioning using an epidemic-type aftershock model. Int. J. Rock Mech. Min. Sci. 150, 104975.
Kaiser, P.K., Yazici, S., Maloney, S., 2001. Mining-induced stress change and consequences of stress path on excavation stability-a case study. Int. J. Rock Mech. Min. Sci. 38 (2), 167–180.
Kang, H.P., Lv, H.W., Gao, F.Q., Meng, X.Z., Feng, Y.J., 2018. Understanding mechanisms of destressing mining-induced stresses using hydraulic fracturing. Int. J. Coal Geol. 196, 19–28.
Kastner, H., 1971. Statik des Tunnel- und Stollenbau. Auf Der Grundlage Geomechnischer Erkenntnisse. Springer Berlin, Heidelberg (in German).
Li, Y.Y., Harianto, R., Alfrendo, S., Saranya, R., Daryl, T.T.L., 2022. Soil database development with the application of machine learning methods in soil properties prediction. Eng. Geol. 306, 106769.
Ludeña-Choez, J., Choquehuanca-Zevallos, J.J., Mayhua López, E., 2019. Sensor nodes fault detection for agricultural wireless sensor networks based on NMF. Comput. Electron. Agric. 161, 214–224.
Mikhail, E., Gabriel, E., Igor, S., 2020. Numerical simulation of roof cavings in several Kuzbass mines using finite-difference continuum damage mechanics approach. Int. J. Rock Mech. Min. Sci. 30 (2), 157–166.
Mohammad, A., Mohammad, K., Robert, G.P.J., 2021. A new framework to deal with the class imbalance problem in urban gain modeling based on clustering and ensemble models. Geocarto Int. 37 (19), 5669–5692.
Mohammad, R., Mohammad, F.H., Abbas, M., 2015. Development of a time-dependent energy model to calculate the mining-induced stress over gates and pillars. J. Rock Mech. Geotech. Eng. 7 (3), 306–317.
Prasanjit, D., Chaulya, S.K., Kumar, S., 2021. Hybrid CNN-LSTM and IoT-based coal mine hazards monitoring and prediction system. Process Saf. Environ. Protect. 152, 249–263.
Prosper, E.A.A., Sylvanus, S.N., Jessica, W.A.A., et al., 2022. A review and case study of Artificial intelligence and Machine learning methods used for ground condition prediction ahead of tunnel boring Machines. Tunn. Undergr. Space Technol. 125, 104497.
Protodyakonov, M.M., 1907. Rock Pressure on Mine Support. Tipografiya Gubernskogo Zemstva, Yekaterinoslav (in Russian).
Qian, M.G., Liu, T.C., 1984. Ground Pressure and its Control. China Coal Industry Publishing House, Beijing (in Chinese).
Qin, C.K., Zhao, W.S., Zhong, K., Chen, W.Z., 2022. Prediction of longwall mining-induced stress in roof rock using LSTM neural network and transfer learning method. Energy Sci. Eng. 10, 458–471.
Rami, A., Gabriel, W., Sankhaneel, S., 2020. Understanding roof deformation mechanics and parametric sensitivities of coal mine entries using the discrete element method. Int. J. Rock Mech. Min. Sci. 30 (1), 123–129.
Tan, X.Y., Chen, W.Z., Tan, X.J., Zou, T., Du, B.W., 2022a. Prediction for the future mechanical behavior of underwater shield tunnel fusing deep learning algorithm on SHM data. Tunn. Undergr. Space Technol. 125 (7), 104504.
Tan, X.Y., Chen, W.Z., Zou, T., Yang, J.P., Du, B.W., 2022b. Real-time prediction of mechanical behaviors of underwater shield tunnel structure using machine learning method based on structural health monitoring data. J. Rock Mech. Geotech. Eng. https://doi.org/10.1016/j.jrmge.2022.06.015.
Tan, X.Y., Sun, X.X., Chen, W.Z., Du, B.W., Ye, J.C., Sun, L.L., 2021a. Investigation on the data augmentation using machine learning algorithms in structural health monitoring information. Struct. Health Monit. 20 (4), 2054–2068.
Tan, X.Y., Chen, W.Z., Wu, G.J., Wang, L.Y., Yang, J.P., 2020. A structural health monitoring system for data analysis of segment joint opening in an underwater shield tunnel. Struct. Health Monit. 19 (4), 1032–1050.
Tan, X.Y., Wang, Y.H., Du, B.W., et al., 2021b. Analysis for full face mechanical behaviors through spatial deduction model with real-time monitoring data. Struct. Health Monit. 21 (4), 1805–1818.
Teng, Y.Y., Yao, Y.D., Qi, S.L., et al., 2019. A novel framework for the NMF methods with experiments to unmixing signals and feature representation. J. Comput. Appl. Math. 362, 205–218.
Terzaghi, K., 1943. Theoretical Soil Mechanics. John Wiley & Sons, New York.
Vitor, S.B., Claudio, R., 2020. A simplified estimation procedure for the Weibull stress parameter, m, and applications to predict the specimen geometry dependence of cleavage fracture toughness. Int. J. Pres. Ves. Pip. 188, 104228.
Wang, L.Y., Chen, W.Z., Tan, X.Y., et al., 2020. Numerical investigation on the stability of deforming fractured rocks using discrete fracture networks: a case study of underground excavation. Bull. Eng. Geol. Environ. 79, 133–151.
Wang, L.Y., Chen, W.Z., Tan, X.Y., Yang, J.P., 2019. The impact of various crack geometrical parameters on stress field over tip under different mixed loading conditions and inclination angles. Theor. Appl. Fract. Mech. 102, 239–254.
Wang, S.Y., Si, G.Y., Wang, C.B., et al., 2022. Quantitative assessment of the spatio-temporal correlations of seismic events induced by longwall coal mining. J. Rock Mech. Geotech. Eng. 14 (5), 1406–1420.
Xie, H.P., Zhou, H.W., Liu, J.F., Gao, F., 2011. Mining-induced mechanical behavior in coal seams under different mining layouts. J. China Coal Soc. 36 (7), 1067–1074 (in Chinese).
Zhang, Z.T., Xie, H.P., Zhang, R., Gao, M.Z., Ai, T., Zha, E.S., 2020. Size and spatial fractal distributions of coal fracture networks under different mining-induced stress conditions. Int. J. Rock Mech. Min. Sci. 132, 104364.
Zhao, W.S., Zhong, K., Chen, W.Z., 2020. A fiber Bragg grating borehole deformation sensor for stress measurement in coal mine rock. Sensors 20 (11), 3267.
Zhu, H.H., Azarafaza, M., Akgün, H., 2022. Deep learning-based key-block classification framework for discontinuous rock slopes. J. Rock Mech. Geotech. Eng. 14 (4), 1131–1139.

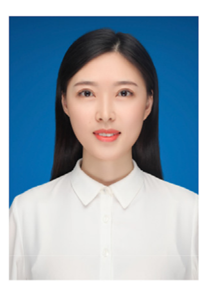

Dr. Xuyan Tan obtained her BSc degree in Safety Engineering from Shandong University of Science and Technology, China, in 2016, and her PhD in Geotechnical Engineering from Institute of Rock and Soil Mechanics, Chinese Academy of Sciences, China, in 2021. She is now working as a research assistant professor in Institute of Rock and Soil Mechanics, Chinese Academy of Sciences. Her research interests include (1) intelligent monitoring for the spatio-temporal mechanical behaviors of underground engineering; and (2) the application of deep learning technology in the analysis of structural mechanical response, anomaly diagnosis, and early warning in the field.